Ultra-high-resolution CT to detect intracochlear new bone formation after cochlear implantation

Heutink, F.; Klabbers, T.M.; Huinck, W.J.; Lucev, F.; Woude, W.J. van der; Mylanus, E.A.M.; Verbist, B.M.

Radiology

ORIGINAL RESEARCH • HEAD AND NECK IMAGING

Ultra-High-Resolution CT to Detect Intracochlear New Bone Formation after Cochlear Implantation

*Floris Heutink, MD** • *Tim M. Klabbers, MD** • *Wendy J. Huinck, PhD* • *Federica Lucev, MD* • *Willem Jan van der Woude, BSc* • *Emmanuel A. M. Mylanus, MD, PhD* • *Berit M. Verbist, MD, PhD*

From the Departments of Otorhinolaryngology (F.H., T.M.K., W.J.H., E.A.M.M.) and Radiology (W.J.v.d.W., B.M.V.), Radboud University Medical Center, Philips van Leydenlaan 16, Route 377, PO Box 9101, 6500 HB Nijmegen, the Netherlands; Donders Institute for Brain, Cognition and Behaviour, Nijmegen, the Netherlands (F.H., T.M.K., W.J.H., E.A.M.M.); Department of Radiology, Civil Hospital, Vigevano, Italy (F.L.); and Department of Radiology, Leiden University Medical Center, Leiden, the Netherlands (B.M.V.). Received June 3, 2021; revision requested July 28; revision received October 11; accepted October 18. **Address correspondence to** F.H. (e-mail: *Floris.Heutink@radboudumc.nl*).

Supported by an ongoing institutional grant from Cochlear.

* F.H. and T.M.K. contributed equally to this work.

Conflicts of interest are listed at the end of this article.

Radiology 2022; 302:605–612 • https://doi.org/10.1148/radiol.211400 • Content codes: HN CT

Background: Histopathologic studies reported that cochlear implantation, a well-established means to treat severe-to-profound sensorineural hearing loss, may induce inflammation, fibrosis, and new bone formation (NBF) with possible impact on loss of residual hearing and hearing outcome.

Purpose: To assess NBF in vivo after cochlear implantation with ultra-high-spatial-resolution (UHSR) CT and its implication on long-term residual hearing outcome.

Materials and Methods: In a secondary analysis of a prospective single-center cross-sectional study, conducted between December 2016 and January 2018, patients with at least 1 year of cochlear implantation experience underwent temporal bone UHSR CT and residual hearing assessment. Two observers evaluated the presence and location of NBF independently, and tetrachoric correlations were used to assess interobserver reliability. In addition, the scalar location of each electrode was assessed. After consensus agreement, participants were classified into two groups: those with NBF (n = 83) and those without NBF (n = 40). The association between NBF and clinical parameters, including electrode design, surgical approach, and long-term residual hearing loss, was tested using the χ^2 and Student t tests.

Results: A total of 123 participants (mean age ± standard deviation, 63 years ± 13; 63 women) were enrolled. NBF was found in 83 of the 123 participants (68%) at 466 of 2706 electrode contacts (17%). Most NBFs (428 of 466, 92%) were found around the 10 most basal contacts, with an interobserver agreement of 86% (2297 of 2683 contacts). Associations between electrode types and surgical approaches were significant (58 of 79 participants with NBF and a precurved electrode vs 24 of 43 with NBF and a straight electrode, P = .04; 64 of 88 participants with NBF and a cochleostomy approach vs 18 of 34 with NBF and a round window approach, P = .03). NBF was least often seen in full scala tympani insertions, but there was no significant association between scalar position and NBF (P = .15). Long-term residual hearing loss was significantly larger in the group with NBF compared with the group without NBF (mean, 22.9 dB ± 14 vs 8.6 dB ± 18, respectively; P = .04).

Conclusion: In vivo detection of new bone formation (NBF) after cochlear implantation is possible by using ultra-high-spatial-resolution CT. Most cochlear implant recipients develop NBF, predominately located at the base of the cochlea. NBF adversely affects long-term residual hearing preservation.

An earlier incorrect version appeared online. This article was corrected on December 8, 2021.

A cochlear implant is a neuroprosthetic device that forms an effective solution for patients with severe-to-profound hearing loss. Today, even patients with functional residual hearing may receive a cochlear implant. By using soft-surgery techniques (eg, low drill speeds and slow insertion), the extent of insertional trauma can be reduced (1,2). However, long-term changes within the cochlea caused by introducing a foreign body are neither treated nor prevented in current practice (3).

Although cochlear implant electrode arrays are commonly made from biocompatible polymers, they can elicit an inflammatory response in two ways. First, insertional trauma can induce an acute intracochlear tissue response, resulting in formation of iatrogenic scar tissue around the array (4–6). Second, a delayed inflammatory reaction due to the natural host tissue response can lead to encapsulation of the array in a fibrous sheath (7,8). In its most pronounced form, the fibrosis can progress to neo-ossification. This new bone formation (NBF) has been observed in animal and histopathologic studies (5,6,9–13). However, in vivo detection of NBF has not yet been described.

The presence of NBF around the cochlear implant electrode is relevant for several reasons. First, NBF alters the intracochlear electrophysiology. At the electrode contact level, the electrical "impedance" is increased, resulting in higher power consumption and more out-of-compliance issues (14–16). Furthermore, the spread of electrical current within the cochlea is affected, leading to complex device fitting, channel interaction, and poorer worse overall hearing outcome (16). Second, new tissue formation has been theorized to cause long-term residual acoustic hearing loss due to stiffening of the round window membrane and damping of the scala tympani (3). Last, the presence of NBF may complicate future therapies or repeat implantation. Therefore,

Abbreviations

NBF = new bone formation, PTA3 = pure tone average over three frequencies, SVOE = study variable and outcome evaluation, UHSR = ultra high spatial resolution

Summary

Ultra-high-spatial-resolution CT can be used to detect intracochlear new bone formation in vivo following cochlear implantation.

Key Results

- Two radiologists were able to detect new bone formation (NBF) at the individual electrode contact level using ultra-high-spatial-resolution CT, with a mean interobserver agreement of 86% (2297 of 2683 electrode contacts).
- Among the 123 study participants, 83 (68%) had at least one electrode contact with neo-ossification (mean follow-up, 3.8 years after implantation).
- Compared to participants without NBF, participants with NBF were found to have significantly greater long-term residual hearing loss (mean, 22.9 dB vs 8.6 dB, respectively; $P = .04$).

it seems desirable to control and reduce NBF, but this requires a method to detect and monitor NBF in vivo.

Recently, ultra-high-spatial-resolution (UHSR) CT, with 0.25-mm detector elements and matrix size up to 2048, was introduced, showing better delineation of the fine anatomic temporal bone structures than conventional multidetector CT, which has detector elements of 0.5 mm or larger and a matrix size of 512 (17,18). The UHSR CT system has various focal spot sizes, the smallest being of nominal size 0.4×0.5 mm^2 (19), whereas the smallest focus size in standard multidetector CT is 0.8×0.9 mm^2. UHSR CT was used to evaluate intracochlear electrode location, revealing the presence of bone densities alongside the cochlear implant electrode contacts (20).

The primary objective of this study was to describe the amount and location of NBF in a cohort of patients with cochlear implant and to test the reliability of detecting NBF using UHSR CT. The secondary objective was to investigate the association between NBF and two clinical parameters: *(a)* surgical factors (ie, insertion location, electrode type, and intracochlear scalar position) and *(b)* long-term residual hearing loss.

Materials and Methods

This prospective single-center cross-sectional study, conducted between December 2016 and January 2018, was approved by the local and regional medical ethics committees (approval number: NL510071.091.14). All participants signed informed consent. The data set of this study was previously used to find factors associated with cochlear implant speech perception outcome. These results are reported in a separate article (20). The current study is a secondary analysis of this prospective trial.

Study Design

All participants were evaluated for *(a)* the presence and location of postoperative NBF (relative to the implanted electrode), *(b)* the association between NBF and surgical parameters (ie, surgical approach, type of electrode, and intracochlear scalar position), and *(c)* the relationship between NBF and long-term residual hearing loss. The time point of conducting UHSR CT of the temporal bone and measuring the residual hearing was named the "study variable and outcome evaluation" (SVOE). The time between cochlear implant implantation and the SVOE varied, with an average time of 3.8 years (standard deviation, 1.7 years; range, 1.2–7.7 years).

Study Participants

The 129 participants included in this study met the following inclusion criteria: *(a)* postlingual onset of hearing loss, defined as an onset of severe-to-profound hearing loss after the age of 5 years, and *(b)* cochlear implantation between January 2010 and July 2016. Patients with a prelingual onset of hearing loss, cognitive dysfunction, anomalies of the cochleovestibular system at preoperative imaging (CT or MRI), or less than 12 months of experience with cochlear implant were excluded.

CT Technique: Evaluation of NBF

All participants underwent UHSR CT (Aquilion Precision, Canon Medical Systems) at the SVOE. UHSR CT was used to evaluate the presence of NBF. Scans were acquired in sequential scanning mode with a collimation of 160×0.25 mm, resulting in a scan range of 4 cm. The scanning parameters were as follows: 140 kV, 100 mA, rotation time of 1.5 msec, volume CT dose index of 29.9 mGy, and dose-length product of 119.6 mGy · cm, resulting in an effective dose of 0.25 mSv (k factor, 0.0021). Images were reconstructed with filtered back projection in bone kernel (FC81) from images with a 0.25-mm section thickness with every 0.125 mm overlapping, and a field of view of 90 mm with a 1024×1024 matrix, resulting in a pixel spacing of 0.09 mm and a voxel size of $0.09 \times 0.09 \times 0.25$ mm. The scanning parameters were chosen such that image noise—which inherently increases with higher spatial resolution—was ameliorated and artifacts were reduced. With use of axial acquisition, windmill artifacts due to presence of the cochlear implant were averted.

First, oblique multiplanar reconstructions were obtained through the cochlea, parallel to the basal turn of the cochlea. Then, midmodiolar sections were obtained with radial reconstructions through the center of the cochlea (Fig 1). Window width and level were freely adjustable. Two observers (B.M.V. and F.L., with, respectively, 19 years of experience in head and neck radiology and 4 in-training years of experience, of which 1.5 years were focused on subspecialty training in head and neck radiology) independently scored presence of NBF around every cochlear implant electrode contact for each participant. In six participants, image quality was too poor for NBF evaluation owing to movement artifacts (Fig 2). In total, 22 electrode contacts of 123 participants were evaluated (2706 contacts). Each contact identified as located inside the cochlea was scored as either NBF absent or NBF present (Figs 3, 4). The scores of both radiologists were compared and the interobserver reliability calculated using tetrachoric correlations and percentage agreement. The differences in scoring NBF were evaluated and solved during a consensus meeting

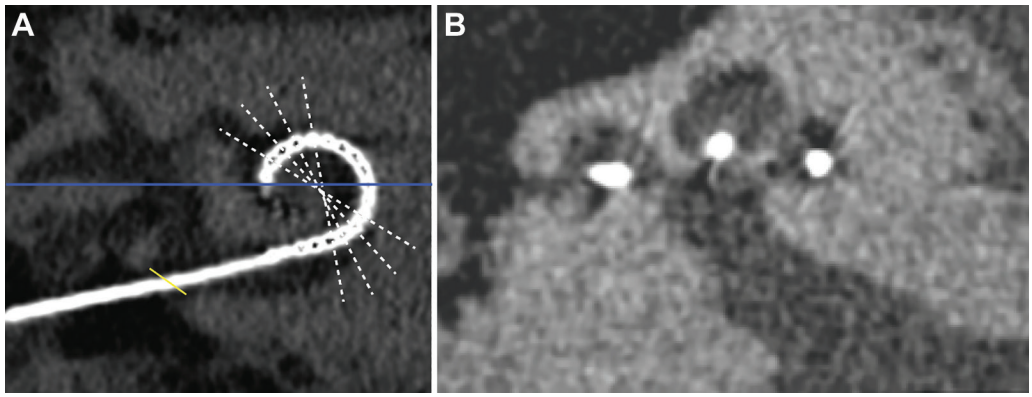

Figure 1: Methods for CT assessment. **(A)** An oblique multiplanar reconstruction through the basal turn of the cochlea was obtained and **(B)** midmodiolar sections were obtained with radial multiplanar reconstruction through the center of the cochlea (white lines in **A**). On such midmodiolar images, the presence or absence of new bone formation and the scalar position were assessed at each electrode contact. Angular insertion depth was measured from the lateral border of the horizontal semicircular canal (blue line in **A**), using a correction factor to the center of the round window (yellow line in **A**) of 34° (21,22).

between the two radiologists. The consensus score was used for further analysis. In addition, scalar location and angular insertion depth of each electrode contact were assessed (Fig 1). The method for both measurements was previously reported (20–22).

Hearing Preservation

The pure tone average over three frequencies (PTA3), defined as the average residual hearing threshold over 500, 1000, and 2000 Hz, was measured in both ears during follow-up at first fitting (ie, 4–6 weeks after surgery) and compared with that at long-term follow-up (ie, during the SVOE). Two residual hearing outcomes were evaluated: *(a)* absolute residual hearing loss (PTA3Diff), defined as the difference between the PTA3 at long-term follow-up (SVOE) and the PTA3 at first fitting (PTA3FirstFit), and *(b)* relative residual hearing preservation percentage (RHP%). We used the hearing preservation classification system of Skarzynski et al (23) to calculate the relative residual hearing preservation percentage, as follows:

$$\mathrm{RHP\%} = \left[1 - \frac{(\mathrm{PTA3Diff})}{(\mathrm{PTA3Max} - \mathrm{PTA3FirstFit})} \cdot 100\right],$$

where PTA3Max is the average maximum stimulation level over the frequencies 500 Hz, 1000 Hz, and 2000 Hz and was the same for all patients (16.7 dB).

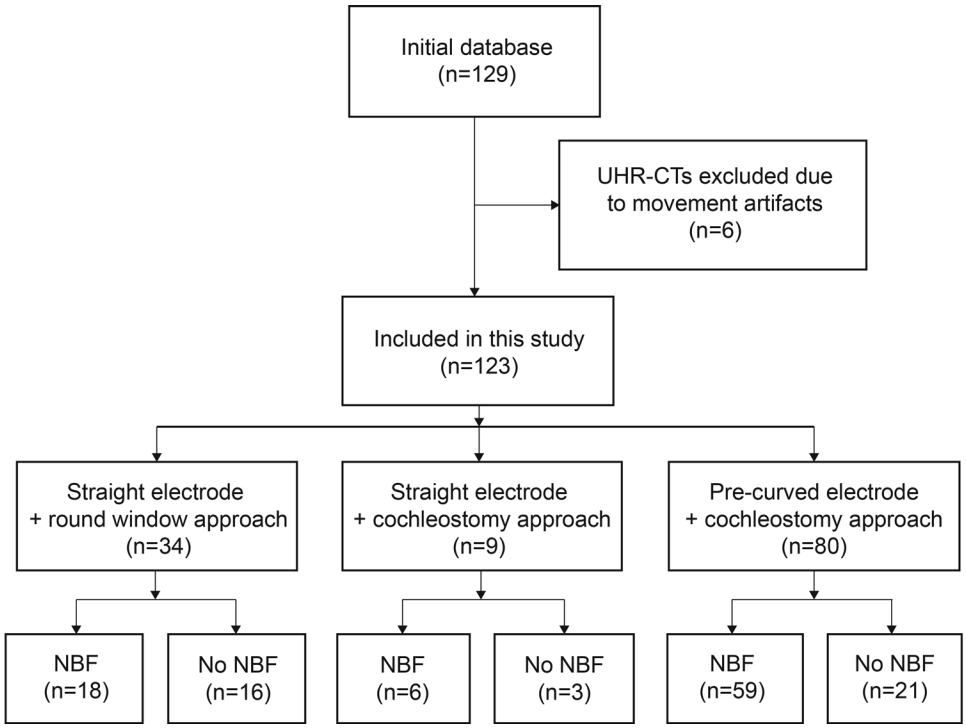

Figure 2: Flowchart of included cochlear implant recipients with ultra-high-spatial-resolution (UHR) CT for evaluation of intracochlear new bone formation (NBF).

Statistical Analysis

Statistical analyses were performed with SPSS software (version 25.0, IBM SPSS). Descriptive data on the amount and location of NBF around all contacts are reported. Tetrachoric correlations were used to determine the interobserver reliability for detecting NBF and were calculated for all intracochlear electrode contacts. Two groups were formed on the basis of the presence of NBF. Associations between NBF groups and categorical variables were tested using the χ^2 test and between NBF and continuous variables using the Student t test. $P < .05$ was considered indicative of a statistically significant difference.

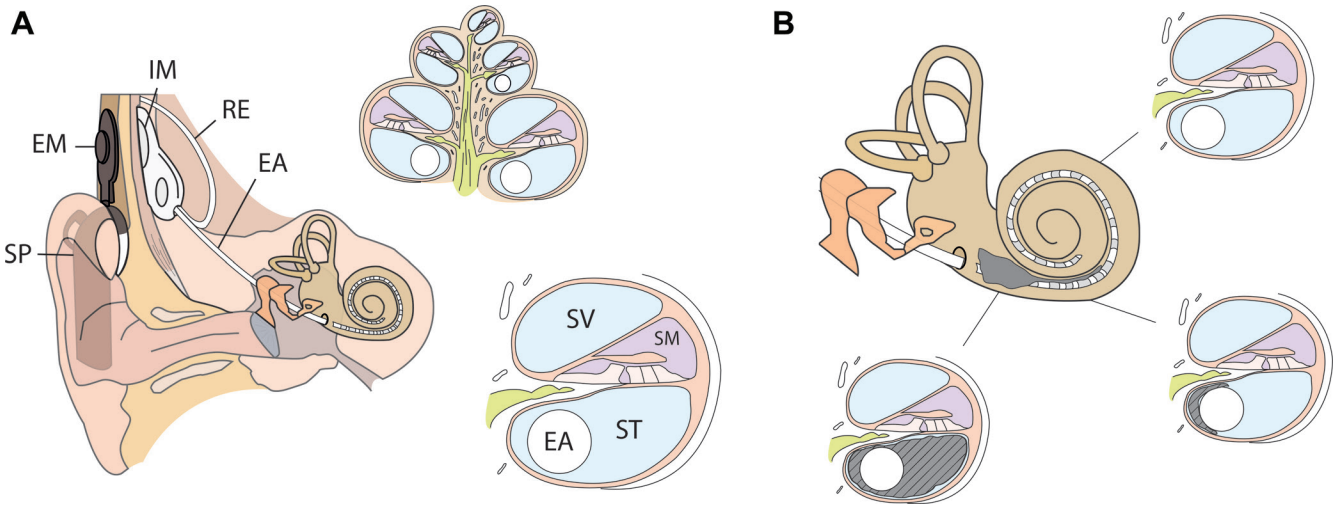

Figure 3: Schematics of **(A)** right ear with cochlear implant, midmodiolar cross-section, and close-up of the different compartments within the cochlea and **(B)** proximal new bone formation (in gray) in the scala tympani (ST) encasing the electrode array (EA), gradually diminishing toward the apex of the cochlea. EM = external magnet, IM = internal magnet, RE = reference electrode, SM = scala media, SP = speech processor, SV = scala vestibuli.

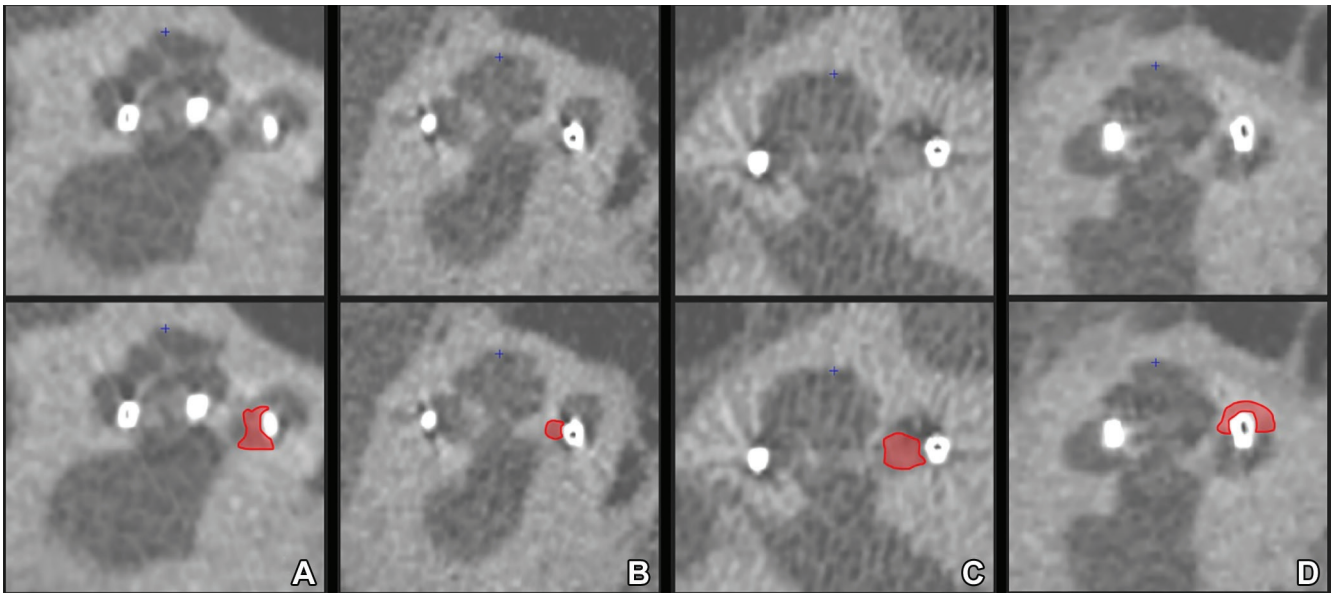

Figure 4: Midmodiolar ultra-high-spatial-resolution CT scans with corresponding annotations indicating new bone formation (NBF) in red. Note the varying appearance of NBF, ranging from **(A)** slightly increased attenuation, resembling that of the modiolus, to **(D)** frank ossification with an attenuation similar to that of the otic capsule surrounding a translocated contact in the scala vestibuli. An intermediate form of NBF appearance is shown in **B** and **C**. Moreover, in **B**, the ossification between the perimodiolar positioned electrode contact and the medial cochlear wall is difficult to discern, resulting in interrater disagreement.

Results

Participant Characteristics

A total of 123 participants who received unilateral cochlear implants at the Radboudumc Cochlear Implant Center, Nijmegen, the Netherlands, were included (mean age ± standard deviation, 63 years ± 13; 63 women). Other demographic and etiologic characteristics can be found in Table 1. All participants received a cochlear implant system from Cochlear. A precurved electrode (Nucleus Contour Advance model CI512/CI24RE) was used for cochlear implant placement in 80 participants and a straight electrode (Nucleus Slim Straight model CI422/522) was used in 43 participants. The precurved electrode was inserted via an antero-inferiorly drilled cochleostomy (n = 80), and the straight electrode was inserted through the round window (n = 34). The round window could not be identified in nine patients in the straight electrode group, and the electrode was inserted with a cochleostomy approach.

NBF Evaluation

The mean interobserver agreement was 86% (2297 of 2683 intracochlear contacts). The interobserver agreement per electrode contact is shown in Table 2. Discrepancies between observers were mainly due to different cutoff points when scoring contacts in the transition zone from evident ossification to fluid-filled cochlear lumen, due to differences in scoring ossification medial to

Table 1: Demographic Data and Hearing Characteristics

Characteristic	Value
No. of participants	123
Sex	
M	60 (48.8)
F	63 (51.2)
Mean age at implantation (y)*	63 ± 13 (27–85)
Implant side	
Right	63 (51.2)
Left	60 (48.8)
Electrode type	
Precurved	80 (65)
Straight	43 (35)
Surgical approach	
Round window	34 (27.6)
Cochleostomy	89 (72.4)
Scalar position of electrode†	
All contacts within scala tympani	58 (47.2)
All contacts within scala vestibuli	27 (22)
Translocation	37 (30.1)
Cause of hearing loss	
DFNA-9	13 (10.5)
Sudden deafness	8 (6.5)
Otosclerosis	4 (3.3)
Usher syndrome	4 (3.3)
Trauma	3 (2.4)
Meniere disease	1 (0.8)
Ototoxic medication	2 (1.6)
Maternal rubella	2 (1.6)
Mumps infection	1 (0.8)
DFNA-22	1 (0.8)
DFNB-3	1 (0.8)
Hereditary, unspecified	25 (20.3)
Unknown	56 (45.5)

Note.—Except where indicated, data are numbers of participants, with percentages in parentheses. DFNA-9 = nonsyndromic hearing loss, autosomal dominant 9; DFNA-22 = nonsyndromic hearing loss, autosomal dominant 22; DFNB-3 = nonsyndromic hearing loss, autosomal recessive 3.

* Data are means ± standard deviation, with ranges in parentheses.

† The quality of six ultra-high-spatial-resolution CT scans was too poor (due to movement artifacts) to score scalar position.

Table 2: Interobserver Agreement per Electrode Contact

Electrode No.	Tetrachoric Correlation Coefficient	No. of Agreements (n = 123)
1	0.78	71 (57.7)
2	0.72	78 (63.4)
3	0.62	76 (61.8)
4	0.71	79 (64.2)
5	0.68	77 (62.6)
6	0.53	81 (65.9)
7	0.75	94 (76.4)
8	0.64	98 (79.7)
9	0.997	111 (90.2)
10	0.79	115 (93.5)
11	0.92	119 (96.7)
12	0.96	120 (97.6)
13	0.89	117 (95.1)
14	0.997	117 (95.1)
15	0.997	117 (95.1)
16	0.998	117 (95.1)
17	0.995	118 (95.9)
18	0.997	120 (97.6)
19	0.99	123 (100)
20	0.99	123 (100)
21	0.99	123 (100)
22	0.99	123 (100)
Mean	0.86	105.3 (85.6)

Note.—Numbers in parentheses are percentages.

the electrode at basal contacts and due to differences in scoring extracochlear contacts at the level of the round window. After consensus between the two radiologists, 68% of the participants (84 of 123) showed one or more electrode contacts with adjacent NBF. Examples of intracochlear NBF with varying densities surrounding the electrode contacts are shown in Figure 4.

The overall prevalence of NBF around all electrode contacts was 17% (466 of 2683 contacts). The distribution of NBF is shown in Figure 5A: 92% of the contacts with NBF (428 of 466) were located around the 10 most basal electrode contacts. On average, contact 10 was located at an angular depth of insertion of 141° (standard deviation, 27°; 95% CI: 136, 146). A total of 79 of the 123 participants (64.2%) had NBF around one of the three first contacts. None of the participants had NBF at the most apical electrode contacts (contacts 21 or 22).

To analyze a possible association between NBF and clinical parameters, participants were classified into two groups: an NBF-positive group and an NBF-negative group. Basal NBF was defined as NBF around one or more of the contacts between an angular insertion depth of 0°–90°. The NBF-positive group consisted of 83 participants with basal NBF, and the NBF-negative group consisted of 40 participants without basal NBF. The associations between basal NBF and surgical parameters, time between cochlear implantation and SVOE, and residual hearing were evaluated.

Surgical Parameters and Time between Cochlear Implant Placement and SVOE

The associations between electrode type and basal NBF and between surgical approach and basal NBF were significant (58 of 79 participants with NBF and precurved electrodes vs 24 of 43 with NBF and straight electrodes, P = .04; 64 of 88 participants with NBF in the cochleostomy group vs 18 of 34 in the round window group, P = .03) but not independent of each other. There were three groups of participants based on electrode type and surgical approach: participants with *(a)* precurved electrode and cochleostomy approach (n = 80), *(b)* straight electrode and rear window approach (n = 34), and *(c)* straight electrode and cochleostomy approach (n = 9). Basal NBF was found in 74% of participants with a

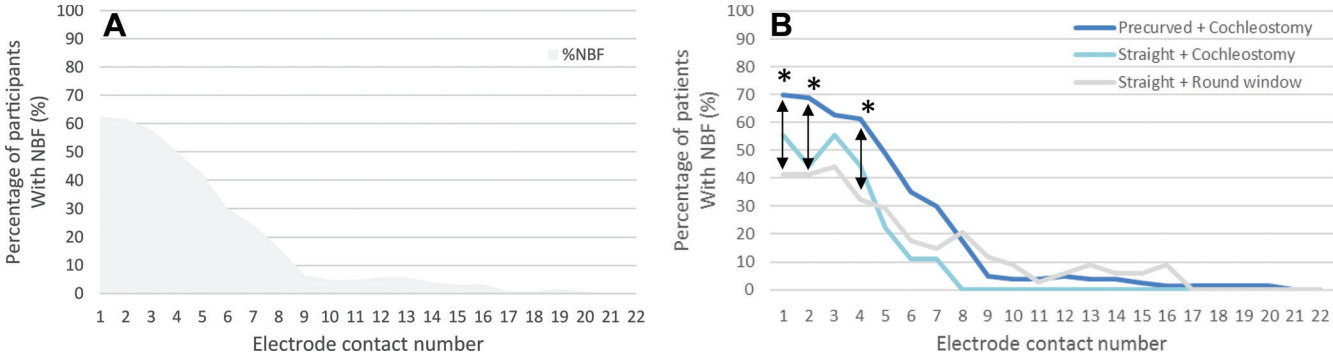

Figure 5: Graphs show percentage of participants with new bone formation (NBF) per electrode contact location **(A)** for all participants and **(B)** according to the three surgical combinations. * = $P < .05$.

precurved electrode and cochleostomy approach (59 of 80), 53% of participants with a straight electrode and rear window approach (18 of 34), and 68% of participants with a straight electrode and cochleostomy approach (six of nine). In Figure 5B, the number of participants with NBF per intracochlear electrode contact is compared among the three groups. For electrode contacts 1, 2, and 4, the number of participants with NBF in the precurved electrode and cochleostomy approach group was significantly higher than that in the straight electrode and rear window approach group (electrode contact 1: 70% [56 of 80 participants] vs 41% [14 of 34 participants], $P = .004$; electrode contact 2: 69% [55 of 80 participants] vs 41% [14 of 34 participants], $P = .006$; electrode contact 4: 61% [49 of 80 participants] vs 32% [11 of 34 participants], $P = .005$). The differences between the precurved electrode and cochleostomy approach group and straight electrode and cochleostomy approach group were not significant ($P > .05$), as can also be observed in Figure 5B.

With regard to scalar position, 59% of the participants with complete scala tympani position (34 of 58) had NBF, whereas 78% (21 of 27) and 73% (27 of 37) of participants with complete scala vestibuli position or translocation had NBF, respectively. This association was not significant ($P = .15$).

The associations between surgical factors and NBF should be interpreted in light of the associations between NBF and time between cochlear implant placement and SVOE (ie, the time between implantation and the measurement of NBF) and the surgical factors and time between cochlear implant placement and SVOE. The mean time between cochlear implant placement and SVOE was 4.14 years ± 1.8 in the NBF-positive group and 3.24 years ± 1.4 in the NBF-negative group ($P = .003$). The time between cochlear implant placement and SVOE was significantly higher in participants with precurved electrode ($P < .001$), cochleostomy approach ($P < .001$), and scala vestibuli position of the electrode ($P = .045$).

Residual Hearing

Participants with a PTA3 higher than 90 dB at first fitting were excluded from residual hearing analysis as they were not considered to have functional residual acoustic hearing. In the residual hearing analysis ($n = 24$), the time since cochlear implant placement was not different between the NBF-positive and NBF-negative groups ($P > .05$).

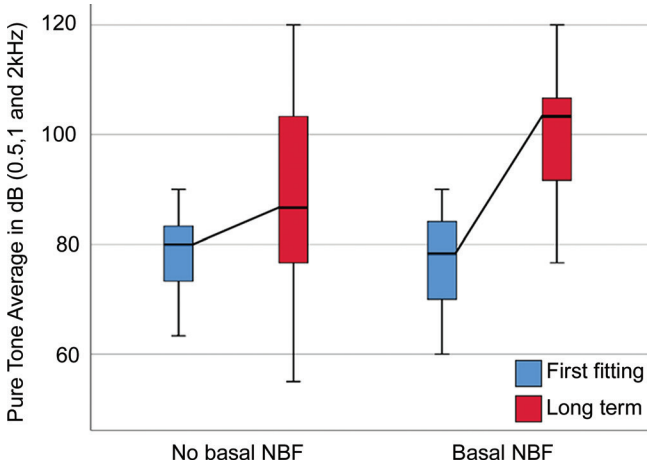

Figure 6: Box plot compares residual acoustic hearing loss in the ear with cochlear implant between the first fitting (the initial activation and calibration of the cochlear implant 4–6 weeks after surgery) and long-term follow-up for participants with and without new bone formation (NBF).

Figure 6 shows the mean threshold of PTA3 in the two NBF groups for the ear with cochlear implant at the two time points during follow-up after cochlear implantation. In the contralateral ear, the mean PTA3 was 54.2 dB ± 13.7 at the first fitting and 60.5 dB ± 18.7 at long-term follow-up, resulting in a PTA3 difference of 6.3 dB in the contralateral ear. Compared with this, a higher decrease of PTA3 threshold is seen in the ear with cochlear implant, especially in the NBF-positive group. The PTA3 difference in the cochlear implant ear was significantly larger in the NBF-positive group compared with the NBF-negative group ($n = 24$, $P = .04$). This long-term residual hearing loss was 22.9 dB ± 14 in the NBF-positive group and 8.6 dB ± 18 in the NBF-negative group. The relative long-term hearing preservation between the first fitting and long-term follow-up was 48.0% for the NBF-positive group and 78.6% for the NBF-negative group; this difference was not significant ($P = .06$; $n = 24$).

Discussion

Several histopathologic postmortem studies reported new bone formation (NBF) after cochlear implant placement and its po-

tential adverse effect on intracochlear electrophysiology and hearing outcome. Our study showed that in vivo detection of NBF after cochlear implant placement is feasible with ultra-high-spatial-resolution (UHSR) CT. UHSR CT doubles the in-plane resolution of multidetector CT systems as a result of smaller detectors (0.25 mm), smaller spot size (0.4–0.5 mm), and larger matrix (up to 2048 × 2048). A low noise level can be maintained with limited increase of dose thanks to detector properties and reconstruction algorithms. The method for in vivo detection of NBF presented in our study was highly reliable, with an interobserver reliability of 86% (2297 of 2683 intracochlear electrodes) (24). NBF was common (68% of participants [84 of 123], 17% of all electrode contacts [466 of 2683]) and mostly located around the 10 most basal contacts (92% of the found NBFs [428 of 466]). This mostly basal NBF was associated with a negative effect on long-term residual hearing loss (22.9 dB ± 14 in the NBF-positive group and 8.6 dB ± 18 in the NBF-negative group; $P = .04$; $n = 24$).

The interobserver reliability between the two radiologists was highest in apical regions with minimal or no NBF, implying best agreement on the absence of NBF. NBF is a gradual process from slight fibrosis to dense bone, reflected in different tissue attenuations on CT scans, while the method described herein uses a binary score. During the consensus meeting between the two radiologists, most discrepancies were found at the contacts lying in the gradual transition zone from evident bone formation to a fluid-filled cochlear lumen.

In three histopathologic studies investigating NBF in patients with cochlear implant, all 39 temporal bones studied showed some degree of NBF (5,6,9). Compared with this, our study showed a lower prevalence of NBF. There may be several possible reasons for this. First, our method is less precise compared with histopathologic evaluation. The development of NBF is a gradual transition from mild fibrosis to dense bone (5,6,9–13). Richard et al (25) showed that the density of intracochlear tissue may range from translucent (areolar) fibrosis to dense fibrosis to neo-ossification. This is reflected in variable attenuation of NBF at UHSR CT. Low-attenuation new tissue formation may not be detected with UHSR CT. Second, the follow-up period in years since implantation in our study was shorter than in histopathologic studies. Although the time needed for NBF to develop is unclear, a delayed inflammatory reaction may continue for several years after implantation. Finally, developments in surgical technique may have decreased the risk of traumatic insertion and NBF. Considering the publication dates and duration of cochlear implant use reported in the histopathologic studies, the time frame of implantation seems to be between 1995 and 2005. In this period, the soft-surgery technique used in the present study was uncommon.

Although the amount of NBF differs, the predominantly basal location of NBF is in accordance with previous publications. This suggests an association with trauma due to opening of the cochlea. However, associations found between the surgical factors investigated in this study and NBF were not strong and covaried strongly with time between cochlear implant placement and SVOE. Although trends were found indicating more NBF in patients with a precurved electrode and those with partially or completely translocated implants, findings should be interpreted cautiously given the longer follow-up time and potential other factors contributing to intralabyrinthine new tissue formation.

We found a negative effect of NBF on long-term residual hearing. The loss of residual hearing was found in the low frequencies, whereas one might expect basal NBF to cause high-frequency hearing loss, considering the cochlear tonotopic organization. This mismatch indicates that the effect of NBF on residual hearing is likely to be a cochlea-wide process. Although this might be the result of a direct negative influence of NBF on residual hearing due to inflammation, oxidative stress, and apoptosis of hair cells throughout the cochlea, it is also possible that it is caused by an inner ear conductive hearing loss due to NBF impeding sound transduction through the cochlea, affecting hearing across all frequencies.

Our study had several limitations. First, there was no reference standard to confirm the presence of NBF. Second, although CT parameters were optimized for artifact and noise reduction, further improvement may be possible with the use of hybrid-iterative reconstruction (AIDR 3D Enhanced, Canon Medical Systems). Third, the interval between implantation and UHSR CT varied between participants. This may have led to underestimation of NBF as it is unclear how long it takes for NBF to develop. In the residual hearing analysis ($n = 24$), differences in time between cochlear implant placement and SVOE were not significant between the groups with and without NBF ($P > .05$), but the sample size was small ($n = 24$).

In conclusion, our results indicate that in vivo detection of new bone formation (NBF) using ultra-high-spatial-resolution CT is possible, and that the majority of cochlear implant recipients are likely to develop NBF after cochlear implantation. This neo-ossification was predominately located at the base of the cochlea and seems to be associated with surgical parameters that are considered more traumatic. Long-term residual hearing loss was more pronounced in patients with intracochlear bone formation.

Author contributions: Guarantors of integrity of entire study, **F.H., T.M.K., W.J.H., E.A.M.M., B.M.V.**; study concepts/study design or data acquisition or data analysis/interpretation, all authors; manuscript drafting or manuscript revision for important intellectual content, all authors; approval of final version of submitted manuscript, all authors; agrees to ensure any questions related to the work are appropriately resolved, all authors; literature research, **F.H., T.M.K., W.J.H., E.A.M.M., B.M.V.**; clinical studies, all authors; experimental studies, **F.H., T.M.K., W.J.H.**; statistical analysis, **F.H., T.M.K., W.J.H.**; and manuscript editing, **F.H., T.M.K., W.J.H., W.J.v.d.W., E.A.M.M., B.M.V.**

Disclosures of conflicts of interest: **F.H.** Institutional grants from Cochlear Benelux and Med-El; patents planned, issued, or pending from Cochlear Worldwide. **T.M.K.** Institutional grant from Cochlear Benelux and Med-El. **W.J.H.** Investigator-initiated research fund from Cochlear Benelux and Med-El; support for attending meetings and/or travel from Med-El. **F.L.** No relevant relationships. **W.J.v.d.W.** No relevant relationships. **E.A.M.M.** Investigator-initiated research fund from Cochlear Benelux and Med-El; honoraria for lectures and presentations from Cochlear; support for attending meetings and/or travel from Cochlear and Med-El; participation on data safety monitoring board or advisory board for Cochlear. **B.M.V.** Investigator-initiated research from Cochlear Benelux and Med-El; institutional grants from Advanced Bionics; patents pending from Cochlear; leadership or fiduciary role in other board, society, committee or advocacy group, unpaid, from European Society of Head and Neck Radiology.

References

1. Banakis Hartl RM, Kaufmann C, Hansen MR, Tollin DJ. Intracochlear Pressure Transients During Cochlear Implant Electrode Insertion: Effect of Micro-mechanical Control on Limiting Pressure Trauma. Otol Neurotol 2019;40(6):736–744.
2. Friedland DR, Runge-Samuelson C. Soft cochlear implantation: rationale for the surgical approach. Trends Amplif 2009;13(2):124–138.
3. Foggia MJ, Quevedo RV, Hansen MR. Intracochlear fibrosis and the foreign body response to cochlear implant biomaterials. Laryngoscope Investig Otolaryngol 2019;4(6):678–683.
4. Ishai R, Herrmann BS, Nadol JB Jr, Quesnel AM. The pattern and degree of capsular fibrous sheaths surrounding cochlear electrode arrays. Hear Res 2017;348:44–53.
5. Kamakura T, Nadol JB Jr. Correlation between word recognition score and intracochlear new bone and fibrous tissue after cochlear implantation in the human. Hear Res 2016;339:132–141.
6. Li PM, Somdas MA, Eddington DK, Nadol JB Jr. Analysis of intracochlear new bone and fibrous tissue formation in human subjects with cochlear implants. Ann Otol Rhinol Laryngol 2007;116(10):731–738.
7. Anderson JM, Rodriguez A, Chang DT. Foreign body reaction to biomaterials. Semin Immunol 2008;20(2):86–100.
8. Sheikh Z, Brooks PJ, Barzilay O, Fine N, Glogauer M. Macrophages, Foreign Body Giant Cells and Their Response to Implantable Biomaterials. Materials (Basel) 2015;8(9):5671–5701.
9. Fayad JN, Makarem AO, Linthicum FH Jr. Histopathologic assessment of fibrosis and new bone formation in implanted human temporal bones using 3D reconstruction. Otolaryngol Head Neck Surg 2009;141(2):247–252.
10. Somdas MA, Li PM, Whiten DM, Eddington DK, Nadol JB Jr. Quantitative evaluation of new bone and fibrous tissue in the cochlea following cochlear implantation in the human. Audiol Neurotol 2007;12(5):277–284.
11. O'Leary SJ, Monksfield P, Kel G, et al. Relations between cochlear histopathology and hearing loss in experimental cochlear implantation. Hear Res 2013;298:27–35.
12. Marsh MA, Jenkins HA, Coker NJ. Histopathology of the temporal bone following multichannel cochlear implantation. Arch Otolaryngol Head Neck Surg 1992;118(11):1257–1265.
13. Nadol JB Jr, Shiao JY, Burgess BJ, et al. Histopathology of cochlear implants in humans. Ann Otol Rhinol Laryngol 2001;110(9):883–891.
14. Clark GM, Shute SA, Shepherd RK, Carter TD. Cochlear implantation: osteoneogenesis, electrode-tissue impedance, and residual hearing. Ann Otol Rhinol Laryngol Suppl 1995;166:40–42.
15. Shaul C, Bester CW, Weder S, et al. Electrical Impedance as a Biomarker for Inner Ear Pathology Following Lateral Wall and Peri-modiolar Cochlear Implantation. Otol Neurotol 2019;40(5):e518–e526.
16. Wilk M, Hessler R, Mugridge K, et al. Impedance Changes and Fibrous Tissue Growth after Cochlear Implantation Are Correlated and Can Be Reduced Using a Dexamethasone Eluting Electrode. PLoS One 2016;11(2):e0147552.
17. Ohara A, Machida H, Shiga H, Yamamura W, Yokoyama K. Improved image quality of temporal bone CT with an ultrahigh-resolution CT scanner: clinical pilot studies. Jpn J Radiol 2020;38(9):878–883.
18. Yamashita K, Hiwatashi A, Togao O, et al. Ultrahigh-resolution CT scan of the temporal bone. Eur Arch Otorhinolaryngol 2018;275(11):2797–2803.
19. Oostveen LJ, Boedeker KL, Brink M, Prokop M, de Lange F, Sechopoulos I. Physical evaluation of an ultra-high-resolution CT scanner. Eur Radiol 2020;30(5):2552–2560 [Published correction appears in Eur Radiol 2020;30(8):4709–4710.].
20. Heutink F, Verbist BM, van der Woude WJ, et al. Factors Influencing Speech Perception in Adults With a Cochlear Implant. Ear Hear 2021;42(4):949–960.
21. Verbist BM, Skinner MW, Cohen LT, et al. Consensus panel on a cochlear coordinate system applicable in histologic, physiologic, and radiologic studies of the human cochlea. Otol Neurotol 2010;31(5):722–730.
22. Verbist BM, Joemai RM, Briaire JJ, Teeuwisse WM, Veldkamp WJ, Frijns JH. Cochlear coordinates in regard to cochlear implantation: a clinically individually applicable 3 dimensional CT-based method. Otol Neurotol 2010;31(5):738–744.
23. Skarzynski H, van de Heyning P, Agrawal S, et al. Towards a consensus on a hearing preservation classification system. Acta Otolaryngol Suppl 2013;133(564):3–13.
24. McHugh ML. Interrater reliability: the kappa statistic. Biochem Med (Zagreb) 2012;22(3):276–282.
25. Richard C, Fayad JN, Doherty J, Linthicum FH Jr. Round window versus cochleostomy technique in cochlear implantation: histologic findings. Otol Neurotol 2012;33(7):1181–1187.

Radiology

Erratum

Originally published in:
https://doi.org/10.1148/radiol.211400

Ultra-High-Resolution CT to Detect Intracochlear New Bone Formation after Cochlear Implantation

Floris Heutink, Tim M. Klabbers, Wendy J. Huinck, Federica Lucev, Willem Jan van der Woude, Emmanuel A. M. Mylanus, Berit M. Verbist

Erratum in:
https://doi.org/10.1148/radiol.219033

Figure 2 contained an error and has been changed to "Pre-curved electrode + **cochleostomy** approach (n=80)."

Radiology

Erratum

Originally published in:
https://doi.org/10.1148/radiol.211400

Ultra-High-Resolution CT to Detect Intracochlear New Bone Formation after Cochlear Implantation

Floris Heutink, Tim M. Klabbers, Wendy J. Huinck, Federica Lucev, Willem Jan van der Woude, Emmanuel A. M. Mylanus, Berit M. Verbist

Erratum in:
https://doi.org/10.1148/radiol.219033

Figure 2 contained an error and has been changed to "Pre-curved electrode + **cochleostomy** approach (n=80)."